

Title	The effect of flexible chains on the orientation dynamics of small molecules dispersed in polymer films during stretching
Author(s)	Nobukawa, Shogo; Aoki, Yoshihiko; Fukui, Yoshiharu; Kiyama, Ayumi; Yoshimura, Hiroshi; Tachikawa, Yutaka; Yamaguchi, Masayuki
Citation	Polymer Journal, 47(4): 294-301
Issue Date	2014-12-24
Type	Journal Article
Text version	author
URL	<a href="http://hdl.handle.net/10119/12868">http://hdl.handle.net/10119/12868</a>
Rights	Copyright (C) 2014 The Society of Polymer Science, Japan. Shogo Nobukawa, Yoshihiko Aoki, Yoshiharu Fukui, Ayumi Kiyama, Hiroshi Yoshimura, Yutaka Tachikawa and Masayuki Yamaguchi, Polymer Journal, 47(4), 2014, 294-301. <a href="http://dx.doi.org/10.1038/pj.2014.126">http://dx.doi.org/10.1038/pj.2014.126</a>
Description	

# The effect of flexible chains on the orientation dynamics of small molecules dispersed in polymer films during stretching

*Shogo Nobukawa<sup>†\*</sup>, Yoshihiko Aoki<sup>†</sup>, Yoshiharu Fukui<sup>†</sup>, Ayumi Kiyama<sup>†</sup>, Hiroshi Yoshimura<sup>‡</sup>, Yutaka Tachikawa<sup>§</sup>, and Masayuki Yamaguchi<sup>†</sup>*

<sup>†</sup>*Japan Advanced Institute of Science and Technology, 1-1 Asahidai, Nomi, Ishikawa 923-1292, Japan,*

<sup>‡</sup>*DIC Corporation, Chiba Plant, 12, Yawata-kaigandori, Ichihara, Chiba 290-8585, Japan,*

<sup>§</sup>*DIC Corporation, Central Research Laboratories, 631, Sakado, Sakura, Chiba 285-8668, Japan*

Running head: Orientation of small molecule in polymer film

\*Corresponding authors:

Shogo Nobukawa

E-mail: nobukawa@jaist.ac.jp

School of Materials Science, Japan Advanced Institute of Science and Technology, 1-1

Asahidai, Nomi, Ishikawa 923-1292, Japan, Tel: +81-761-51-1626

**ABSTRACT**

The effect of flexible chain on orientation dynamics of a small additive molecule in cellulose acetate propionate (CAP) films is investigated during stretching by means of measurements of birefringence and polarized Fourier-transform infrared (FT-IR) spectrum. The orientation birefringence is enhanced by the additives such as ethylene 2,6-naphthalate ( $C_2Np$ ) and hexamethylene 2,6-naphthalate ( $C_6Np$ ) oligomers, suggesting that the additives orient parallel to the CAP chain due to an intermolecular orientation correlation called as the nematic interaction (NI). At a high drawing temperature, the orientation of  $C_2Np$  is stronger than that of  $C_6Np$ , indicating that the flexible alkyl chain reduces the intermolecular NI with CAP. In contrast,  $C_6Np$  orients to the stretching direction rather than  $C_2Np$  at a low temperature. The polarized FT-IR spectra show that the orientation of rigid part in  $C_6Np$  is delayed from that of the flexible group and matrix CAP chain. Consequently, the contribution of  $C_6Np$  to birefringence and its wavelength dependence become stronger with increasing the draw ratio.

Keywords: Additive orientation / Birefringence / Flexible chain / Nematic interaction / Stretching

## INTRODUCTION

Orientation dynamics of polymer chains are strongly related to various kinds of properties such as mechanical, optical, thermal, and dielectric properties.<sup>1-5</sup> In particular, the chain orientation generates an optical anisotropy, namely, birefringence, which is important for optical applications, such as liquid crystal displays, electro luminescence displays, and optical pick-up lenses. In order to improve the performance of these devices, both birefringence value and its wavelength dependence are necessarily controlled. For example, quarter-wave plate, which is one of the most important optical films, is required to exhibit a retardation of a quarter of wavelength for the wide range of visible lights. However, in general, such optical properties cannot be provided in a conventional film using a single polymer component.

When polymer films are stretched beyond a glass transition temperature ( $T_g$ ), the orientation birefringence,  $\Delta n$ , is induced.  $\Delta n$  is defined to be the difference between the two refractive indices in the directions parallel and perpendicular to the stretching direction, i.e.,  $n_{//}$  and  $n_{\perp}$ , respectively,  $\Delta n = n_{//} - n_{\perp}$ . The orientation birefringence  $\Delta n$  is proportional to the degree of the chain orientation,  $F$ , as follows.<sup>6</sup>

$$\Delta n(\lambda) = \Delta n^0(\lambda)F \quad (1)$$

Here,  $\Delta n^0$  is an intrinsic birefringence where the anisotropic molecule perfectly orients to the stretching direction. As represented in equation 1,  $\Delta n^0$  is dependent on the wavelength,  $\lambda$ , while  $F$  is independent. Therefore, for polymer films composed of single component, the wavelength dependence of  $\Delta n$ ,  $\Delta n(\lambda)/\Delta n(\lambda_0)$ , cannot be changed by the chain orientation as represented by,

$$\frac{\Delta n(\lambda)}{\Delta n(\lambda_0)} = \frac{\Delta n^0(\lambda)}{\Delta n^0(\lambda_0)} = \text{const.} \quad (2)$$

In order to control the birefringence and its wavelength dependence for optical films, a combination of double or multi components having different wavelength dependence is applicable. Various techniques such as blending with other polymers<sup>7,8</sup> or small molecules<sup>9-12</sup>, copolymerization<sup>13-15</sup>, and sheet piling<sup>16</sup> have been considered. For the industrial applications, blending with small molecules is easier and more suitable than the other methods due to the following reasons. For polymer blending and copolymerization, the number of combination of materials is limited due to the poor miscibility of polymer pairs. For lamination, the thermal expansion mismatch between polymer sheets restricts the temperature range of use.

The orientation birefringence of the blend,  $\Delta n_{blend}$ , is expressed by a simple addition rule given by,

$$\begin{aligned}\Delta n_{blend}(\lambda) &= \sum \Delta n_i(\lambda) \\ &= \sum \phi_i \Delta n_i^0(\lambda) F_i\end{aligned}\tag{3}$$

where  $\phi_i$ ,  $\Delta n_i^0$ , and  $F_i$  are volume fraction, intrinsic birefringence, and orientation function for component  $i$ . As shown in Figure 1, the birefringence and its wavelength dependence of the blend are determined by the component birefringences. Especially, concentration and orientation function of the components contribute to the birefringence as represented by equation 3. Since the small molecules reduce the thermal resistance of polymer films due to the plasticization effect, the additive content is limited. Contrary, the additive orientation is originated by an intermolecular orientation correlation, which is called as a nematic interaction (NI).<sup>17, 18</sup> The orientation function of additives,  $F_{add}$ , is proportional to that of matrix polymer,  $F_{poly}$ , suggesting that the wavelength dependence cannot be controlled by the stretching condition if the orientation dynamics of additives are completely coupled with that of the matrix polymer chain. However, if the additive orientation is independently generated from the matrix polymer, the wavelength dependence can be modified for the blend films with the same composition.

[Figure 1]

Choudhury et al.<sup>19</sup> investigated the orientation dynamics of poly(ethylene terephthalate) (PET) with high molecular weight by using  $^1\text{H}$ - $^{13}\text{C}$  cross-polarization magic-angle-spinning (CP/MAS) NMR spectroscopy. According to them, ethylene part in PET exhibits 10 times shorter relaxation time than phenyl ring, indicating that the orientation of the flexible chain is induced by stretching prior to the orientation of the rigid part. Therefore, for small molecules with similar structure to PET, the flexible and rigid parts might exhibit different orientation time in polymer films during stretching, leading to the control of the wavelength dependence for birefringence.

In this study, the effect of alkyl chains on the orientation dynamics of small additives in polymer films during stretching is investigated. Two types of alkyl naphthalate as model compounds are mixed with cellulose acetate propionate (CAP), which is used as a model polymer for optical films.<sup>20</sup> Especially, the detail of additive orientations in CAP films is investigated by using the birefringence measurement and Fourier-transform infrared (FT-IR) spectroscopy.

## **EXPERIMENTAL**

### **Samples**

CAP (Figure 2) was produced by Eastman Chemical Company (TN, USA). The weight-average and number-average molecular weights ( $M_w$  and  $M_n$ ) of CAP were  $2.1 \times 10^5$  and  $7.7 \times 10^4$ , respectively, determined by a gel-permeation-chromatography (GPC, HLC-8020 Tosoh, Japan) with a polystyrene standard. Degrees of substitution for acetyl and propionyl groups per a pyranose unit of CAP are 0.19 and 2.58, respectively. Ethylene 2,6-naphthalate) and hexamethylene 2,6-naphthalate oligomers ( $C_2Np$  and  $C_6Np$ , Figure 2) used as additives were synthesized from alkane diol and dimethyl naphthalene 2,6-dicarboxylate (DMNDC) as following reactions. DMNDC and ethylene glycol (EG) (or 1,6-hexamethylene diol, HD) with an excess molar quantity against DMNDC were mixed in a flask. After adding tetraisopropyl titanate as a catalyst for the esterification reaction into the flask, the mixture was stirred at 200 °C for half a day under a nitrogen atmosphere. Finally, by removing the residual EG (or HD) at 200 °C in vacuo,  $C_2Np$  or  $C_6Np$  was obtained. The number-average molecular weight ( $M_n$ ) was calculated from the fraction of hydroxyl group at the chain end in a molecule, which was estimated using a method of end-group determination with potassium hydrate. The melting temperature ( $T_m$ ) of the additives was evaluated by a differential scanning calorimeter (DSC-822e, Mettler Toleda Int. Inc., Switzerland). The values of  $M_n$  and  $T_m$  are summarized in Table 1. As shown in the table, the degrees of polymerization of  $C_2Np$  or  $C_6Np$  are slightly different (1.3 and 1.6,



respectively).

Blends of CAP and C<sub>2</sub>Np (or C<sub>6</sub>Np) at a weight ratio of 100/10 wt/wt were prepared by using a 60 cc batch-type internal mixer (Labo-plastmil, Toyoseiki, Japan) at 200 °C for 6 min with the blade rotation speed of 30 rpm. The preparation condition was determined as explained in our previous paper.<sup>21</sup> In order to avoid chemical reactions such as hydrolysis degradation and trans-esterification, CAP was dried in vacuo at 80 °C for 2 hours before melt-mixing. After being kept in a vacuum oven at room temperature for at least one day, the blend samples were compressed into sheets with a thickness of 20-30 μm at 200 °C for 5 min under 10 MPa by a compression-molding machine (Table-type-test press SA-303-I-S, Tester Sangyo, Japan) and were subsequently cooled down at 25 °C for 5 min.

[Figure 2]

[Table 1]

## Measurements

Dynamic mechanical analysis (DMA) for the sample films was carried out to determine tensile storage and loss moduli ( $E'$  and  $E''$ , respectively) at 10 Hz as a function of temperature by a tensile oscillatory rheometer (DVE-E4000, UBM, Japan)

from 25 to 180 °C with a heating rate of 2 °C min<sup>-1</sup>.

DSC was operated to evaluate the crystallinity in CAP and CAP/additive films during a first heating process with a heating rate of 10 °C min<sup>-1</sup>.

A hot-stretching test for the films was carried out with a strain rate of 0.05 s<sup>-1</sup> by using a tensile drawing machine (DVE-3, UBM, Japan). The stretching temperatures were determined from the DMA data, where the tensile modulus is 10 or 100 MPa at 10 Hz. The films were immediately quenched by cold air blowing after stretching to avoid relaxation of molecular orientation.

The stretched films were kept in a humidic chamber (IG420, Yamato, Japan) at 25 °C and 50 %RH for one day in order to prevent moisture effect on birefringence data as reported in a previous paper.<sup>22</sup> During the stock process in the chamber, the chain orientation of CAP does not relax because glass transition temperatures ( $T_g$ 's) are much higher than the storage temperature even for CAP/additive blends. The birefringence of the drawn films was measured as a function of wavelength by using an optical birefringence analyzer (KOBRA-WPR, Oji Scientific Instruments, Japan).<sup>23</sup>

In order to evaluate orientation functions ( $F$ ) for CAP, C<sub>2</sub>Np and C<sub>6</sub>Np in the stretched films, polarized Fourier-transformed infrared (FT-IR) spectra were measured over the scan range of 400 - 4000 cm<sup>-1</sup> with a resolution of 4 cm<sup>-1</sup> at room temperature by using an FT-IR spectrometer (Jasco. Inc., Japan) equipped with a wire-grid polarizer.

The detail of the measurement for molecular orientation is explained in supplementary information.

## RESULTS and DISCUSSION

### Miscibility and plasticization of CAP by additives

Figure 3 shows the dynamic mechanical property of CAP and CAP/additive blends in temperature range of 0 to 180 °C. The glass transition temperature ( $T_g$ ) defined as the peak temperature of loss modulus  $E''$  was determined to be 146, 119 and 116 °C for bulk CAP, CAP/C<sub>2</sub>Np and CAP/C<sub>6</sub>Np, respectively, as listed in Table 2. Both blends showed broader glass transition than bulk CAP, meaning that the relaxation time distribution for the glass transition becomes wider by the addition of C<sub>2</sub>Np and C<sub>6</sub>Np. This phenomenon, which is explained by a concentration fluctuation theory, has been reported in many polymer blends including plasticized polymers.<sup>24-26</sup> The distribution of concentration in the systems is related to the broadness of the glass transition. Furthermore, the reduction of  $T_g$  by C<sub>2</sub>Np and C<sub>6</sub>Np on CAP are the same degree, which might be due to the similarity of chemical structure and molecular weight as shown in Figure 2 and Table 1.

[Figure 3]

[Table 2]

In the rubbery region above  $T_g$ , CAP/additive blends show the same level (~10 MPa) of storage modulus  $E'$  with the bulk CAP. In general, the rubbery plateau modulus for crystalline polymers such as cellulose acetate is 100 MPa.<sup>27, 28</sup> However, as shown in Figure 4, DSC curves for the films show no melting peak, which could appear from 150 to 200 °C for CAP used in this study<sup>23</sup>, suggesting that the crystalline content is negligibly small for CAP in bulk and blend films.

[Figure 4]

### **Stress-strain behavior of CAP and CAP/additive films**

Stretching polymer films induces chain orientation, which originates tensile stress  $\sigma$  and birefringence  $\Delta n$ . According to the stress-optical rule represented in equation 4, the following relation between  $\Delta n$  and  $\sigma$  is obtained.

$$\Delta n = C\sigma \quad (4)$$

Considering equation 1,  $\sigma$  is proportional to the orientation function  $F$  as well as  $\Delta n$ , i.e.,

the chain orientation can be controlled by the stress level.

Prior to stretching CAP and CAP/additive films, two drawing temperatures ( $T_{\text{draw}}$ ) were determined from storage modulus in Figure 3 following the previous paper.<sup>20</sup> As shown in Table 2, the gap between  $T_{\text{draw}}$  and  $T_g$  becomes larger by additives because the glass transition is broadened as seen in Figures 3 and 4. Figure 5 shows the stress-strain (S-S) curves of CAP and CAP/additive films at two  $T_{\text{draw}}$ 's ( $T_{10\text{MPa}}$  or  $T_{100\text{MPa}}$ ). For CAP films, the stress levels are much different between  $T_{10\text{MPa}}$  and  $T_{100\text{MPa}}$ . However, as explained later, the orientation function of CAP is similar between the two draw temperatures while it depends on the draw ratio, meaning that the orientation behavior of CAP chain is insensitive to temperature within the experimental condition in this study. This might be because the tensile stress at the lower temperature ( $T_{100\text{MPa}}$ ) contains the glassy stress related to the local distortion in CAP chain as well as the rubbery stress originated from the chain orientation, as reported by Maeda and Inoue.<sup>29</sup> Consequently, the rubbery stress is almost similar between the two draw temperatures, meaning that the difference in orientation function of CAP is small.

[Figure 5]

By comparing S-S curves in Figure 5, the three films exhibit the same level of tensile stress at  $T_{10\text{MPa}}$ . Contrary, at  $T_{100\text{MPa}}$ , the stress value for CAP/C<sub>2</sub>Np is slightly larger than those for CAP and CAP/C<sub>6</sub>Np. However, the orientation functions of CAP in bulk and blend films is almost similar because the rubbery stresses are not so different, as mentioned above for pure CAP. The same level of orientation function suggests that the orientation birefringence of CAP is similar between bulk and blend. Therefore, the difference in orientation birefringence between CAP and CAP/additive is originated from the additive orientation as previously discussed.<sup>20</sup>

### **Orientation birefringence of stretched CAP/additive films**

Figure 6 shows the orientation birefringence  $\Delta n$  of CAP and CAP/additive films stretched at two drawing temperatures. In the figure,  $\Delta n$  values of all samples monotonically increase with the draw ratio as well as the tensile stress  $\sigma$  shown in Figure 5. By comparing Figures 5 and 6, however, the curves of  $\Delta n$  against draw ratio are obviously different from that of  $\sigma$  for bulk and blend. In general, since both  $\sigma$  and  $\Delta n$  of amorphous polymers at the rubbery state are originated from the chain orientation, the two curves against draw ratio should be the same as predicted from Equation 4. In contrast, according to Yamaguchi et al.<sup>23</sup>,  $\Delta n$  for CAP is generated by the alignment of substitution groups, which are acetyl and propionyl groups, because the polarizability

anisotropy of a pyranose ring in the main chain is negligibly small. Furthermore, since the alignments of acetyl and propionyl groups are not completely cooperative with the main chain orientation at higher draw ratio, the curves of  $\sigma$  and  $\Delta n$  were different for CAP and CAP/additive blends, as shown in Figures 5 and 6.

[Figure 6]

In Figure 6, the  $\Delta n$  values of CAP/additive films are larger than that of the CAP film, indicating that the additive molecules contribute  $\Delta n$  as represented by equation 3. It is shown in Figure 6(A), the effect of C<sub>2</sub>Np is stronger than that of C<sub>6</sub>Np for  $\Delta n$  at  $T_{10\text{MPa}}$ . However, Figure 6(B) at  $T_{100\text{MPa}}$  indicates that the enhancement by C<sub>6</sub>Np is almost similar to that by C<sub>2</sub>Np. This result demonstrates that the contribution of the additives to  $\Delta n$  depends on the drawing temperature. As reported in our previous papers<sup>20, 21</sup>, the enhancement of birefringence is generated by the additive orientation, which is induced by the chain orientation of surrounding polymers, i.e., the intermolecular NI. Therefore, the effect of the drawing temperature on the orientations of C<sub>2</sub>Np and C<sub>6</sub>Np in CAP is compared.

Figure 7 compares the wavelength dependence of  $\Delta n$  for CAP and CAP/additive films stretched at various draw ratios. As reported by Yamaguchi et al.<sup>23</sup>,

the CAP film shows extraordinary wavelength dispersion, in which  $\Delta n$  increases with wavelength, and the slope of curve becomes larger with increasing draw ratio. On the other hand, CAP/additive films except for CAP/C<sub>6</sub>Np at  $T_{10\text{MPa}}$  exhibit ordinary wavelength dispersion, where  $\Delta n$  decreases with wavelength. Furthermore, the wavelength dependence is affected by the additive species. In the case of CAP/C<sub>2</sub>Np film, the wavelength dependence of  $\Delta n$  is independent of the draw ratios in this study. Contrary, for CAP/C<sub>6</sub>Np film, the wavelength dependence slightly changes from extraordinary to ordinary with increasing draw ratio, suggesting that the additive orientation is slower than the chain orientation of CAP during stretching.

[Figure 7]

According to equations 2 and 3, the wavelength dependence of  $\Delta n$  in binary blend films is determined from the ratio of two components. Since the wavelength dependence for CAP becomes stronger with the draw ratio, the result for CAP/C<sub>2</sub>Np in Figure 7(B), where the wavelength dependence does not change, suggests that the contribution of C<sub>2</sub>Np to birefringence is enhanced more at larger draw ratios. Additionally, the wavelength dispersion for CAP/C<sub>6</sub>Np was changed from extraordinary to ordinary at large draw ratios, meaning that the contribution of C<sub>6</sub>Np becomes



stronger during stretching as in the case of CAP/C<sub>2</sub>Np. These results might be related to the difference in the time/strain required for the orientation of CAP chains and additives because it depends on the temperature. In order to discuss the orientation dynamics of C<sub>2</sub>Np and C<sub>6</sub>Np in CAP films at two drawing temperatures, molecular orientation is discussed by polarized FT-IR spectra in the following sections.

### **Molecular orientation of CAP and additives in stretched film**

Polarized FT-IR spectroscopy can investigate orientation function,  $F$ , of CAP and additives in stretched films by using the following equation.

$$F = \frac{R_0 + 1}{R_0 - 2} \frac{R - 1}{R + 2} \quad (5)$$

Here,  $R$  is a ratio of peak intensities,  $A_{\parallel} / A_{\perp}$ . The subscripts of peak absorbance,  $A$ , represent parallel and perpendicular axes to the stretching direction.  $R_0 = 2\cot^2\beta$ , where  $\beta$  is the angle between the transition moment corresponding to the absorption band and the chain axis. The orientation function of CAP,  $F_{\text{CAP}}$ , was evaluated by the peaks at 806 and 884 cm<sup>-1</sup>. Orientations of aromatic part in C<sub>2</sub>Np and C<sub>6</sub>Np were investigated from the peak at 772 cm<sup>-1</sup>. The orientation function of the hexyl chain in C<sub>6</sub>Np was also estimated from the peak at 2860 cm<sup>-1</sup>. The ethylene chain orientation

of C<sub>2</sub>Np cannot be evaluated because the peak of C-H stretching mode appears at the same wavenumber with that for CAP. The analysis of  $F$  values is described in supplementary information.

Figure 8(A) shows the orientation function of CAP,  $F_{884}$ , which was calculated from the peak at  $884\text{ cm}^{-1}$ . The degree of chain orientation,  $F_{884}$ , monotonically increases with the draw ratio, corresponding to the stress-strain curve in Figure 5, because the tensile stress is originated from the chain orientation as mentioned before. Fig.8(A) represents the same level of chain orientation for CAP in the bulk and blend although the degrees of orientation are slightly different between  $T_{10\text{MPa}}$  and  $T_{100\text{MPa}}$ .

[Figure 8]

Figure 8(B) shows the relation between draw ratio and orientation function at  $772\text{ cm}^{-1}$ ,  $F_{772}$ , which represents the orientation of aromatic group in C<sub>2</sub>Np and C<sub>6</sub>Np. As demonstrated in the figure, the orientation of C<sub>2</sub>Np is stronger than that of C<sub>6</sub>Np at  $T_{10\text{MPa}}$  while it is slightly weaker at  $T_{100\text{MPa}}$ . The difference in  $F_{772}$  between C<sub>2</sub>Np and C<sub>6</sub>Np at two temperatures corresponds to the result for birefringence in Figure 6. As mentioned before, the additive orientation ( $F_{add}$ ) is induced by the chain orientation of surrounding polymer ( $F_{poly}$ ) via NI<sup>18</sup>, as represented by the following equation.

$$F_{add} = \left[ \frac{\phi_{poly} \varepsilon_{poly,add}}{1 - \phi_{poly} \varepsilon_{poly,poly}} \right] F_{poly} \quad (6)$$

Here,  $\phi$  is a volume fraction and  $\varepsilon_{ij}$  is the NI parameter between components  $i$  and  $j$ .

Since  $\phi_{poly}$  and  $\varepsilon_{poly,poly}$  are constants for the samples in this study, the degree of additive orientation  $F_{add}$  ( $=F_{722}$ ) is determined by only the intermolecular NI represented by  $\varepsilon_{poly,add}$ . Therefore, the additive orientation due to the NI can be discussed with the ratio,  $F_{add}/F_{poly}$  ( $=F_{772}/F_{884}$ ).

### Orientation dynamics of C<sub>2</sub>Np and C<sub>6</sub>Np induced by NI

Prior to investigate the orientation dynamics of the additives in CAP, the effect of molecular weight is commented. In our previous paper<sup>20</sup>, the effect of molecular weight on the orientation of alkyl terephthalate oligomers in CAP was discussed. According to the paper, for higher degree of polymerization ( $n$ ) than 2, the orientation function of the additive oligomers becomes larger with increasing the  $n$  value. However, for lower value of  $n$  (1 or 2), the additive orientation is almost similar. According to the result, in this study, since the  $n$  values of C<sub>2</sub>Np and C<sub>6</sub>Np are lower than 2 (1.3 and 1.6, respectively), the effect of  $n$  on the orientation dynamics can be

ignored.

In order to discuss the orientation dynamics of C<sub>2</sub>Np and C<sub>6</sub>Np in CAP during stretching,  $F_{772} / F_{884}$  was calculated at various draw ratios as shown in Figure 9. The ratio for CAP/C<sub>2</sub>Np exhibits the same dependence on the draw ratio at  $T_{10\text{MPa}}$  and  $T_{100\text{MPa}}$ , and slightly increases with draw ratio. This result suggests that the C<sub>2</sub>Np orientation is simply generated by the intermolecular NI with the chain orientation of CAP. On the other hand,  $F_{772} / F_{884}$  for CAP/C<sub>6</sub>Np is obviously dependent on the drawing temperature. The ratio,  $F_{772} / F_{884}$  at  $T_{100\text{MPa}}$  is larger than that at  $T_{10\text{MPa}}$  at high draw ratios, leading the difference in the effects of C<sub>6</sub>Np at the two draw temperatures shown in Figure 6. In addition, the ratio at  $T_{100\text{MPa}}$  increases with the draw ratio, indicating that the orientation of the aromatic group in C<sub>6</sub>Np, which corresponds to the FT-IR peak at  $772\text{ cm}^{-1}$ , is delayed from the chain orientation of CAP at  $T_{100\text{MPa}}$ .

[Figure 9]

Choudhury et al.<sup>19</sup> investigated chain dynamics of poly(ethylene terephthalate) (PET) with high molecular weight by using  $^1\text{H}$ - $^{13}\text{C}$  cross-polarization magic-angle-spinning (CP/MAS) NMR spectroscopy. They explained that the

relaxation time of the phenyl ring in PET is 10 times as long as that of the ethylene group, suggesting that the rigid and flexible parts have the different time/strain required for the orientation. Since the additive molecules in this study also have similar structure to PET, the above result is applicable for the discussion of orientation dynamics in this study.

The orientation of flexible part in C<sub>2</sub>Np cannot be investigated because its FT-IR peak of C-H stretching band is overlapped with that in CAP. On the other hand, the orientation of flexible hexa-methylene group in C<sub>6</sub>Np can be evaluated since the peak locates at different wavenumber from that in the matrix polymer. The orientation functions of rigid and flexible parts in C<sub>6</sub>Np, which are estimated from FT-IR peaks at 772 and 2860 cm<sup>-1</sup>, respectively, are shown in Figure 10. At higher drawing temperature ( $T_{10\text{MPa}}$ ),  $F_{772}$  and  $F_{2860}$  are comparable, meaning that the flexible and rigid parts in C<sub>6</sub>Np have the same orientation time in stretched CAP film. However, at lower temperature ( $T_{100\text{MPa}}$ ),  $F_{772}$  becomes close to  $F_{2860}$  with increasing the draw ratio, implying that the aromatic group in the C<sub>6</sub>Np molecule has longer relaxation time than the alkyl chain. This orientation behavior of C<sub>6</sub>Np is similar to the chain dynamics of PET reported by Choudhury et al.

[Figure 10]

As shown in Figure 9, the orientation of C<sub>6</sub>Np at low temperature ( $T_{100\text{MPa}}$ ) was stronger than that at high temperature ( $T_{10\text{MPa}}$ ). This phenomenon was also reported for other types of additives in our previous paper.<sup>20</sup> The orientation behavior of additives is explained as follows. According to the nematic interaction (NI) theory, the additive orientation is induced by the chain orientation of matrix polymers due to the intermolecular NI, i.e., orientation coupling. Therefore, the additive orientation ( $F_{\text{add}}$ ) should be cooperative with or delayed from the chain orientation of matrix polymer ( $F_{\text{poly}}$ ), meaning that the ratio of orientation functions,  $F_{\text{add}}/F_{\text{poly}}$  becomes smaller at lower temperatures because the relaxation time of additives becomes longer. However, at low temperature, the glassy stress generates the local chain distortion of polymers, which might enhance the flexible chain alignment such as the *trans* formation of polyethylene chain. Actually, in the experimental data, the orientation of the flexible part (hexa-methylene group) in C<sub>6</sub>Np at  $T_{100\text{MPa}}$  is stronger than that at  $T_{10\text{MPa}}$ . For C<sub>2</sub>Np, the flexible part is too short to induce the orientation at  $T_{100\text{MPa}}$ . The alignment of flexible part enhances the orientation of rigid part in C<sub>6</sub>Np, especially at  $T_{100\text{MPa}}$  as shown in Figure 9.

Based on the above discussion, a following model is considered to explain the orientation dynamics of C<sub>6</sub>Np in CAP film. Firstly, the chain orientation of CAP

induces the alignment of flexible parts in C<sub>6</sub>Np. At low temperature near  $T_g$ , the local chain distortion originated from the glassy stress also generates the flexible chain orientation. Secondly, the rigid (aromatic) part orients after the flexible part orientation due to the difference in orientation relaxation times. As the result, the wavelength dependence of birefringence for CAP/C<sub>6</sub>Np was changed during stretching as shown in Figure 7(C). In general, the wavelength dependence of orientation birefringence of optical polymers is hardly controlled by processing conditions. However, as discussed in this study, the wavelength dependence in polymer blend can be modified by adjusting the drawing conditions for the orientation dynamics of additive molecules.

## Conclusions

In order to control the wavelength dependence of orientation birefringence for cellulose acetate propionate (CAP) film, we investigated the orientations of small additive molecules in CAP films during stretching. In order to examine the effect of flexible chains on the orientation dynamics, two types of additives, 2,6-ethylene naphthalate (C<sub>2</sub>Np) and 2,6-hexamethyl naphthalate (C<sub>6</sub>Np) oligomers, were used in this study.

The birefringence of CAP/additive film was larger than that of pure CAP film,

indicating that the additive orientation is generated due to an orientation correlation represented by an intermolecular nematic interaction (NI). Furthermore, C<sub>2</sub>Np improved the birefringence of CAP more than C<sub>6</sub>Np at higher drawing temperature. However, at lower temperatures, C<sub>6</sub>Np showed stronger enhancement of birefringence than C<sub>2</sub>Np. This result suggests that the orientation of C<sub>6</sub>Np is generated more than that of C<sub>2</sub>Np at the lower temperatures. The wavelength dependence of birefringence for CAP/C<sub>6</sub>Np film was gradually changed from extraordinary to ordinary, indicating that the orientation dynamics of C<sub>6</sub>Np is not cooperative with the chain orientation of CAP although the orientation is induced by the NI.

From polarized FT-IR spectra, the orientation function of CAP, C<sub>2</sub>Np and C<sub>6</sub>Np were evaluated. Especially, for C<sub>6</sub>Np, orientations of the hexa-methylene group and the aromatic ring were not coupled during stretching at lower temperatures. This result suggests that the flexible part in C<sub>6</sub>Np oriented prior to the alignment of the rigid part, i.e., the different orientation time of the flexible and rigid parts in alkyl naphthalate molecules. By applying this phenomenon, birefringence and its wavelength dependence of polymer films containing additives could be controlled even in the same blend films.



## **Acknowledgement**

This work was partly supported by a Grant-in-Aid for Young Scientists B (25870268), and by a grant from the Kyoto Technoscience Center in 2013.

Supplementary information is available at Polymer Journal's website.

## REFERENCES

1. McCrum, N. G., Read, B. E. & Williams, G., *Anelastic and Dielectric Effects in Polymeric Solids*. (Dover Publications, Inc., New York, 1967).
2. Doi, M. & Edwards, S. F., *The Theory of Polymer Dynamics*. (Oxford University Press, New York, 1986).
3. Harding, G. F., *Optical Properties of Polymers*. (ed. Meeten, G. H.), (Elsevier Applied Science Publishers, London, 1986).
4. Korus, J., Hempel, E., Beiner, M., Kahle, S. & Donth, E., Temperature dependence of alpha glass transition cooperativity. *Acta Polym.* **48**, 369-378 (1997).
5. Taniguchi, N., Urakawa, O. & Adachi, K., Calorimetric study of dynamical heterogeneity in toluene solutions of polystyrene. *Macromolecules* **37**, 7832-7838 (2004).
6. Ward, I. M., The measurement of molecular orientation in polymers by spectroscopic techniques. *J. Poly. Sci. Part C Poly. Sym.* **58**, 1-21 (1977).
7. Saito, H. & Inoue, T., Chain orientation and intrinsic anisotropy in birefringence-free polymer blends. *J. Poly. Sci. Part-B Poly. Phys.* **25**, 1629-1636 (1987).
8. Uchiyama, A. & Yatabe, T., Analysis of extraordinary birefringence dispersion of uniaxially oriented poly(2,6-dimethyl 1,4-phenylene oxide)/atactic polystyrene blend films. *Japan J. App. Phys. Part-1* **42**, 3503-3507 (2003).
9. Tagaya, A., Iwata, S., Kawanami, E., Tsukahara, H. & Koike, Y., Zero-birefringence polymer by the anisotropic molecule dope method. *App. Opt.* **40**, 3677-3683 (2001).
10. Tagaya, A., Ohkita, H., Harada, T., Ishibashi, K. & Koike, Y., Zero-birefringence optical polymers. *Macromolecules* **39**, 3019-3023 (2006).
11. Abd Manaf, M. E., Tsuji, M., Shiroyama, Y. & Yamaguchi, M., Wavelength Dispersion of Orientation Birefringence for Cellulose Esters Containing Tricresyl Phosphate. *Macromolecules* **44**, 3942-3949 (2011).
12. Abd Manaf, M. E., Miyagawa, A., Nobukawa, S., Aoki, Y. & Yamaguchi, M., Incorporation of low-mass compound to alter the orientation birefringence in cellulose acetate propionate. *Opt. Mater.* **35**, 1443-1448 (2013).
13. Iwasaki, S., Satoh, Z., Shafiee, H., Tagaya, A. & Koike, Y., Design and synthesis of zero-zero-birefringence polymers in a quaternary copolymerization system. *Polymer* **53**, 3287-3296 (2012).

14. Uchiyama, A., Ono, Y., Ikeda, Y., Shuto, H. & Yahata, K., Copolycarbonate optical films developed using birefringence dispersion control. *Polym. J.* **44**, 995-1008 (2012).
15. Cimrova, V., Neher, D., Kostromine, S. & Bieringer, T., Optical anisotropy in films of photoaddressable polymers. *Macromolecules* **32**, 8496-8503 (1999).
16. Cho, C. K., Kim, J. D., Cho, K., Park, C. E., Lee, S. W. & Ree, M., Effects of the lamination temperature on the properties of poly(ethylene terephthalate-co-isophthalate) in polyester-laminated tin-free steel can - I. Characterization of poly(ethylene terephthalate-co-isophthalate). *J. Adh. Sci. Tech.* **14**, 1131-1143 (2000).
17. Doi, M., Pearson, D., Kornfield, J. & Fuller, G., Effect of nematic interaction in the orientational relaxation of polymer melts. *Macromolecules* **22**, 1488-1490 (1989).
18. Nobukawa, S., Urakawa, O., Shikata, T. & Inoue, T., Evaluation of Nematic Interaction Parameter between Polymer Segments and Low-Mass Molecules in Mixtures. *Macromolecules* **43**, 6099-6105 (2010).
19. Choudhury, R. P., Lee, J. S., Kriegel, R. M., Koros, W. J. & Beckham, H. W., Chain Dynamics in Antiplasticized and Annealed Poly(ethylene terephthalate) Determined by Solid-State NMR and Correlated with Enhanced Barrier Properties. *Macromolecules* **45**, 879-887 (2012).
20. Nobukawa, S., Aoki, Y., Yoshimura, H., Tachikawa, Y. & Yamaguchi, M., Effect of aromatic additives with various alkyl groups on orientation birefringence of cellulose acetate propionate. *J. Appl. Polym. Sci.* **130**, 3465-3472 (2013).
21. Nobukawa, S., Hayashi, H., Shimada, H., Kiyama, A., Yoshimura, H., Tachikawa, Y. & Yamaguchi, M., Strong Orientation Correlation and Optical Anisotropy in Blend of Cellulose Ester and Poly(ethylene 2,6-naphthalate) Oligomer. *J. Appl. Polym. Sci.* **131**, 40570 (2014).
22. Abd Manaf, M. E., Tsuji, M., Nobukawa, S. & Yamaguchi, M., Effect of Moisture on the Orientation Birefringence of Cellulose Esters. *Polymers* **3**, 955-966 (2011).
23. Yamaguchi, M., Okada, K., Abd Manaf, M. E., Shiroyama, Y., Iwasaki, T. & Okamoto, K., Extraordinary wavelength dispersion of orientation birefringence for cellulose esters. *Macromolecules* **42**, 9034-9040 (2009).
24. Hains, P. J. & Williams, G., Molecular motion in polystyrene-plasticizer systems as studied by dielectric relaxation. *Polymer* **16**, 725-729 (1975).

25. Williams, G., Smith, I. K., Aldridge, G. A., Holmes, P. A. & Varma, S., Changes in molecular dynamics during the bulk polymerization of an epoxide/diamine mixture containing inert diluents as studied using dielectric relaxation spectroscopy. *Macromolecules* **34**, 7197-7209 (2001).
26. Lodge, T. P. & McLeish, T. C. B., Self-concentrations and effective glass transition temperatures in polymer blends. **33**, 5278-5284 (2000).
27. Kono, H., Numata, Y., Erata, T. & Takai, M., Structural analysis of cellulose triacetate polymorphs by two-dimensional solid-state C-13-C-13 and H-1-C-13 correlation NMR spectroscopies. *Polymer* **45**, 2843-2852 (2004).
28. Yamaguchi, M., *Optical Properties of Cellulose Esters and Their Blends*. (ed. Lejeune, A. & Deprez, T.), (Nova Science Publishers, New York, 2010).
29. Maeda, A. & Inoue, T., On the Viscoelastic Segment Size of Cellulose. *Nihon Reoroji Gakkaishi* **39**, 159-163 (2011).

## Figure and Table legends

Figure 1. Schematic representation for control of birefringence and its wavelength dependence by additives mixed with matrix polymer.

Figure 2. Chemical structures of CAP and additives.

Figure 3. Temperature dependence of tensile storage and loss moduli ( $E'$  and  $E''$ ) for bulk CAP, and CAP/additive (100/10 wt/wt) films. The oscillatory frequency is 10 Hz and heating rate is 2 °C min<sup>-1</sup>.

Figure 4. DSC curves of CAP and CAP/additive films during heating process with a heating rate of 10 °C/min. The arrows indicate the glass transition temperatures.

Figure 5. Stress-strain curves of CAP and CAP/additive films at two draw temperatures where  $E'$  is 10 or 100 MPa. The strain rate is 0.05 s<sup>-1</sup>.

Figure 6. Orientation birefringence  $\Delta n$  of CAP and CAP/additive (100/10 wt/wt) films stretched with various draw ratios at  $T_{10\text{MPa}}$  and  $T_{100\text{MPa}}$ .

Figure 7. Comparison of wavelength dependence for  $\Delta n$  of CAP and CAP/additive films stretched with various draw ratios at two drawing temperatures.

Figure 8. Orientation functions for (A) CAP and (B) additives in stretched films with various draw ratios at two drawing temperatures.

Figure 9. Ratio of orientation functions for additive and CAP in blend films stretched with various draw ratios at two drawing temperatures.

Figure 10. Ratio of orientation functions for rigid and flexible parts of C<sub>6</sub>Np in blend film stretched with various draw ratios.

Table 1. Molecular weight ( $M_n$ ), degree of polymerization ( $n$ ), melting point ( $T_m$ ), and intrinsic birefringence ( $\Delta n^0$ ) of additives.

Table 2. Glass transition temperature ( $T_g$ ) and drawing temperature ( $T_{\text{draw}}$ ) for CAP and CAP/additive blends.

Table 1. Molecular weight ( $M_n$ ), degree of polymerization ( $n$ ), melting point ( $T_m$ ), and intrinsic birefringence ( $\Delta n^0$ ) of additives.

additive	$M_n$ <sup>a)</sup>	$n$	$T_m$ / °C <sup>b)</sup>	$\Delta n^0$ <sup>c)</sup>
C <sub>2</sub> Np	390	1.3	85	0.14
C <sub>6</sub> Np	643	1.6	97	0.081

a) estimated by a method of end group determination using potassium hydrate

b) determined by DSC

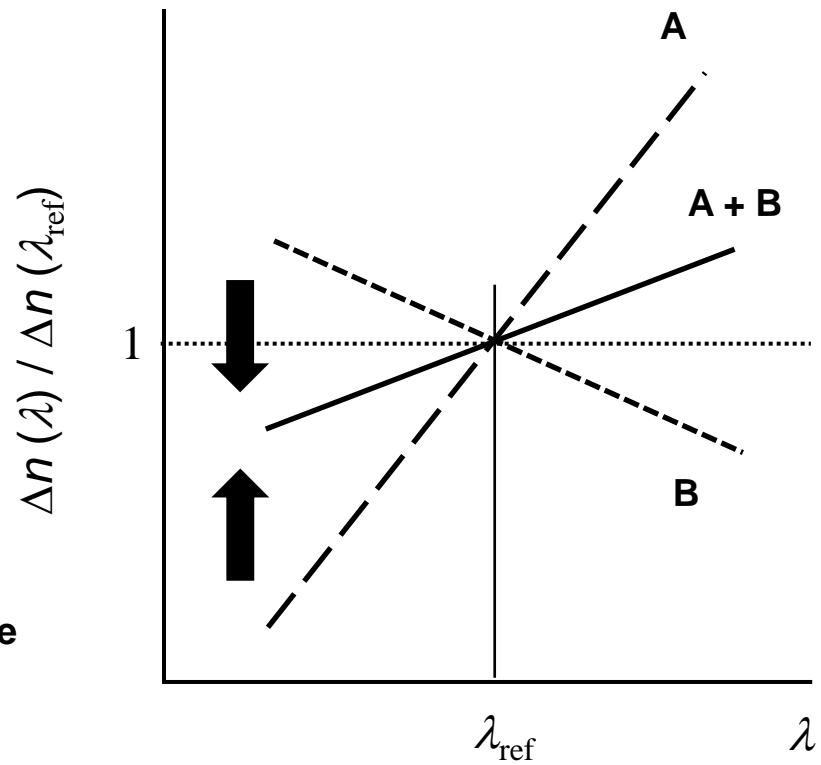
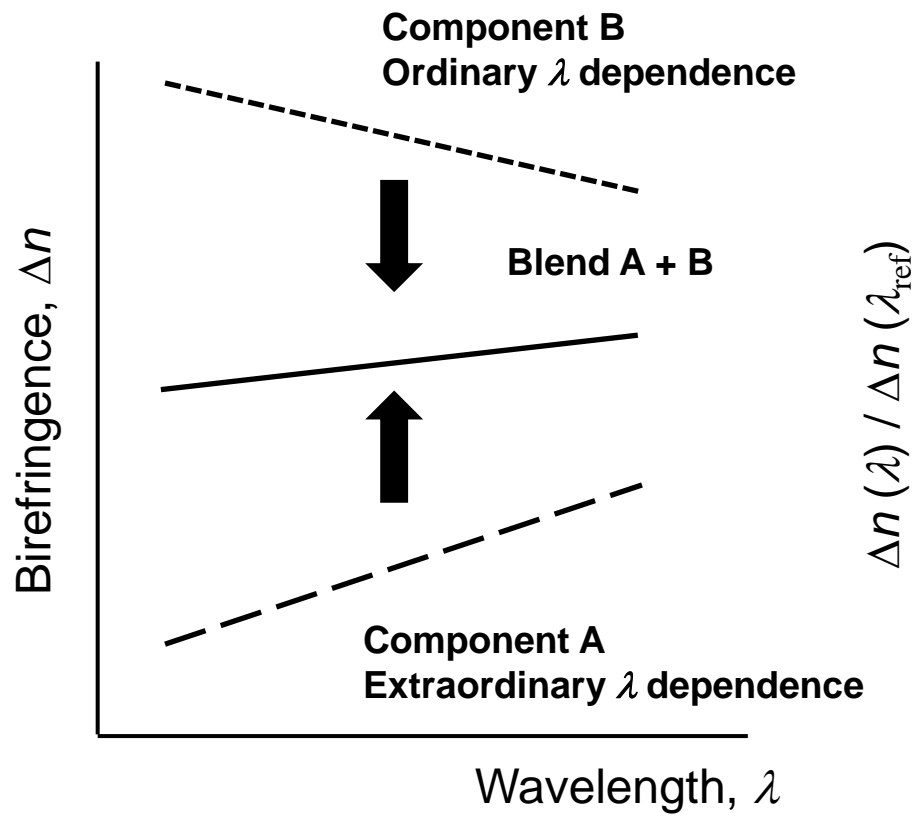
c) calculated by a molecular dynamics simulation with bond-polarizability parameter<sup>21</sup>

Table 2. Glass transition temperature ( $T_g$ ) and drawing temperature ( $T_{\text{draw}}$ ) for CAP and CAP/additive blends.

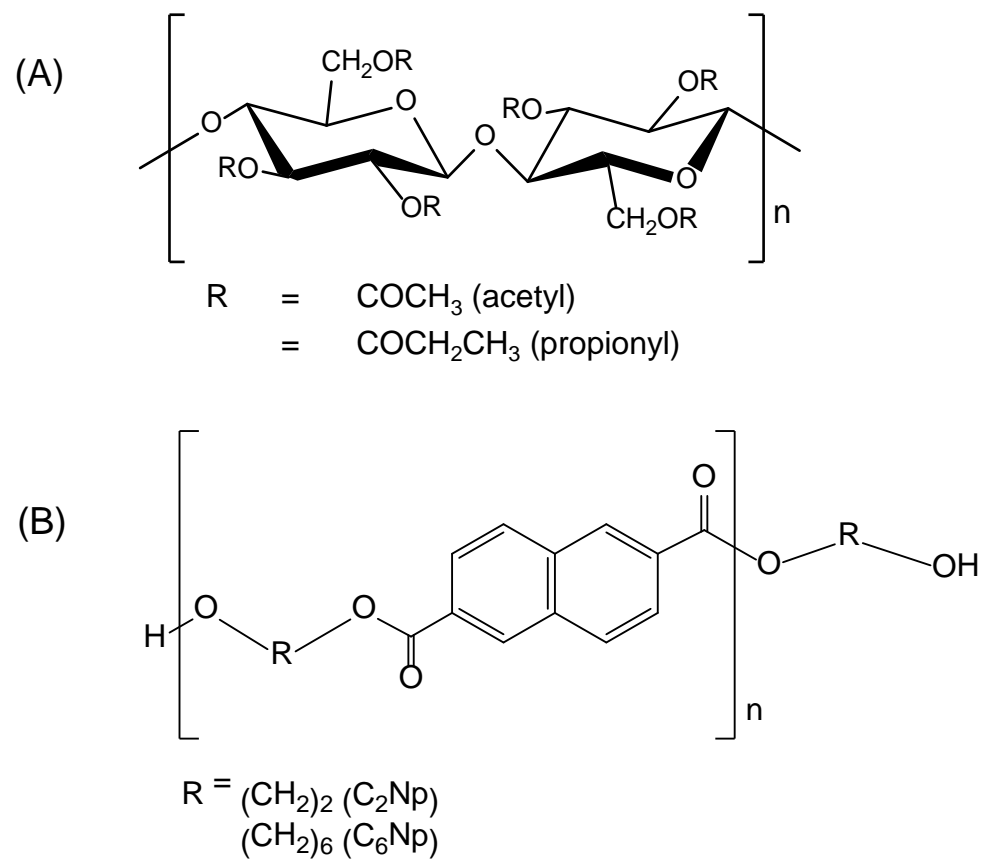
	$T_g / ^\circ\text{C}^{\text{a)}$	$T_{\text{draw}} / ^\circ\text{C}^{\text{b)}$ ( $T_{\text{draw}} - T_g$ )	
		$E' = 10 \text{ MPa}$	$E' = 100 \text{ MPa}$
CAP	146	163 (+17)	152 (+6)
CAP/C <sub>2</sub> Np	119	146 (+27)	127 (+8)
CAP/C <sub>6</sub> Np	116	149 (+33)	133 (+17)

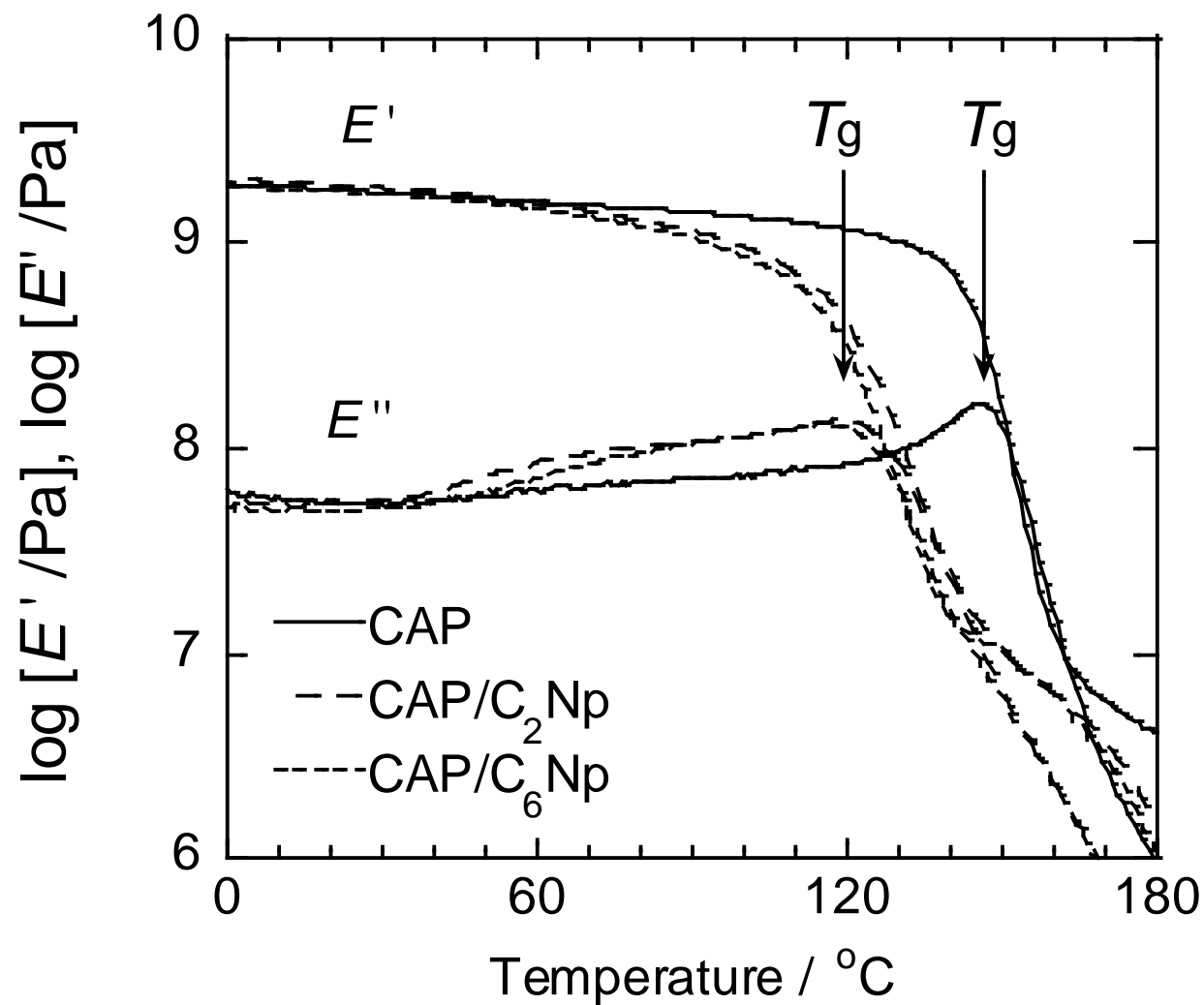
a) defined as a peak temperature of  $E''$  in Figure 3

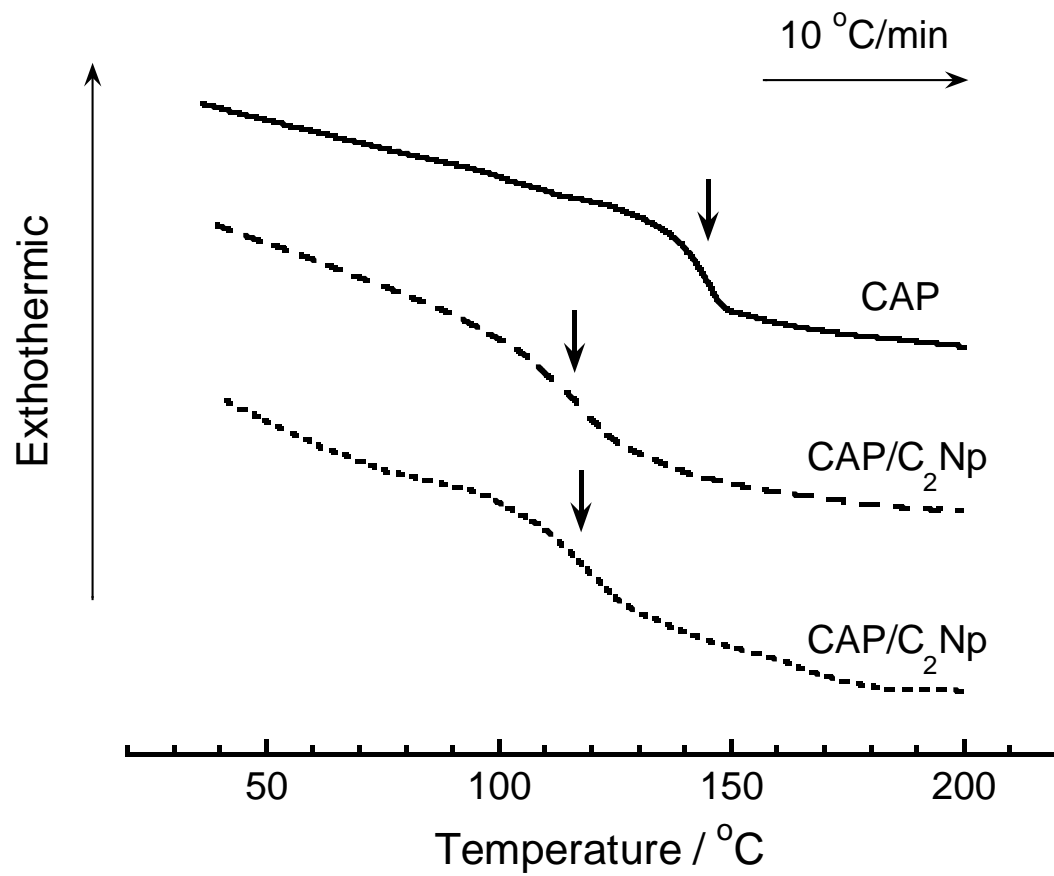
b) determined as a temperature where  $E'$  is 10 or 100 MPa

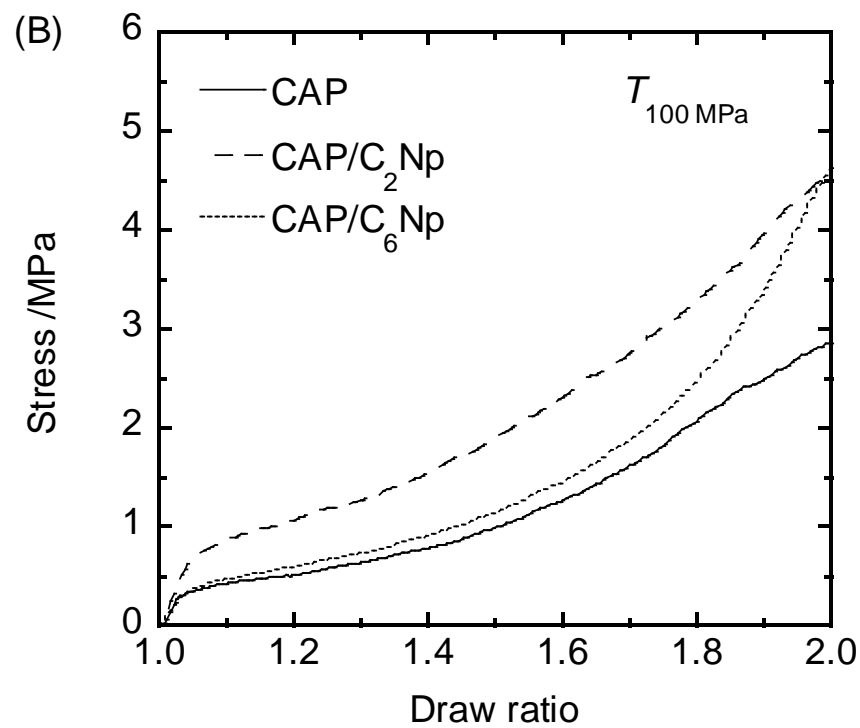
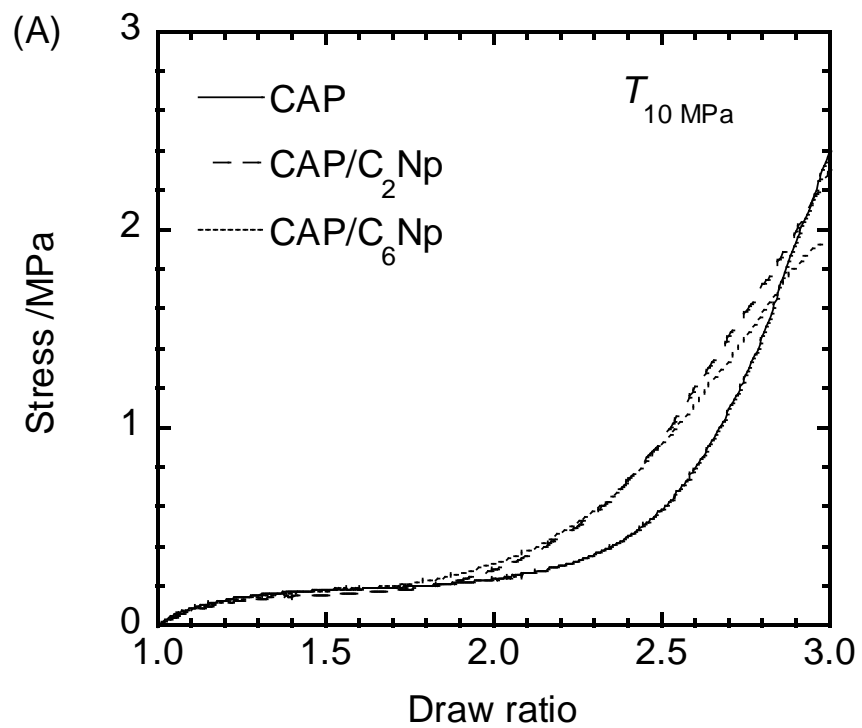


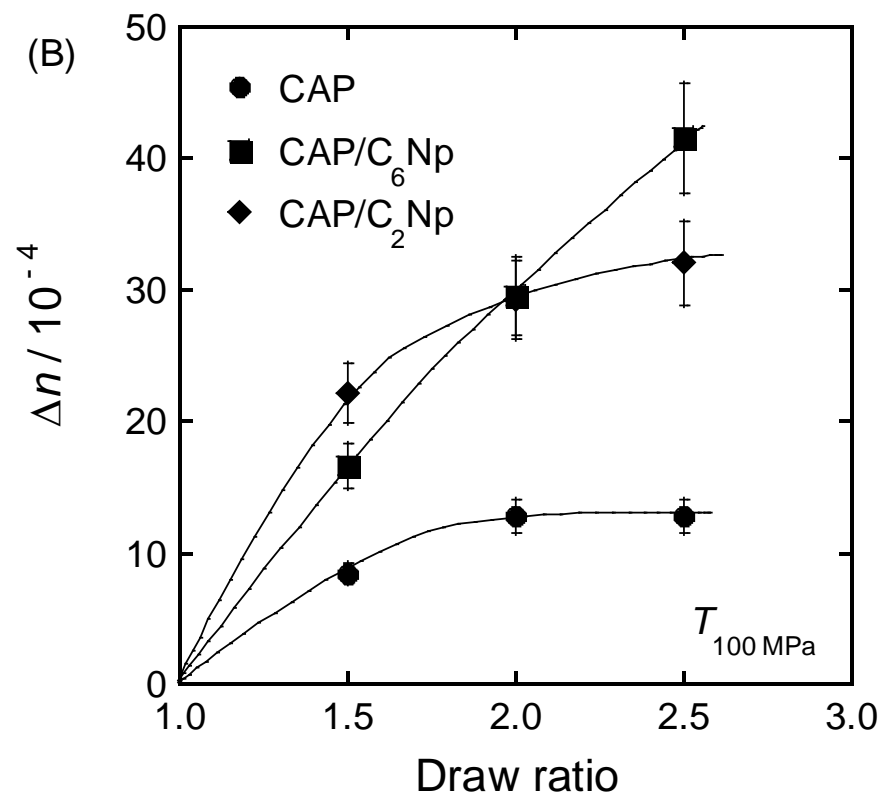
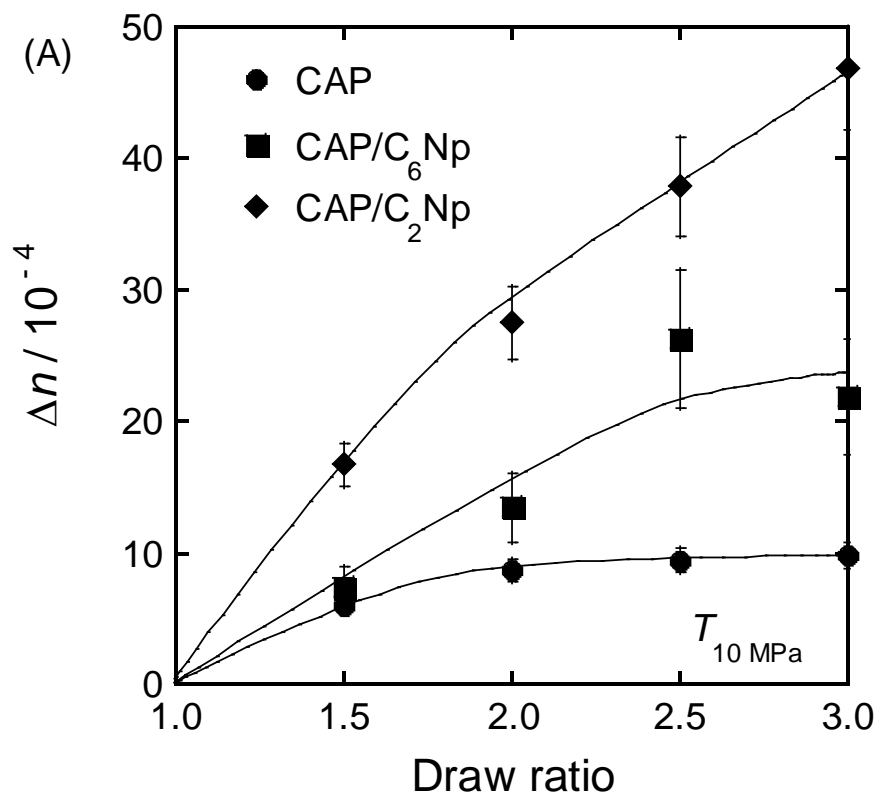


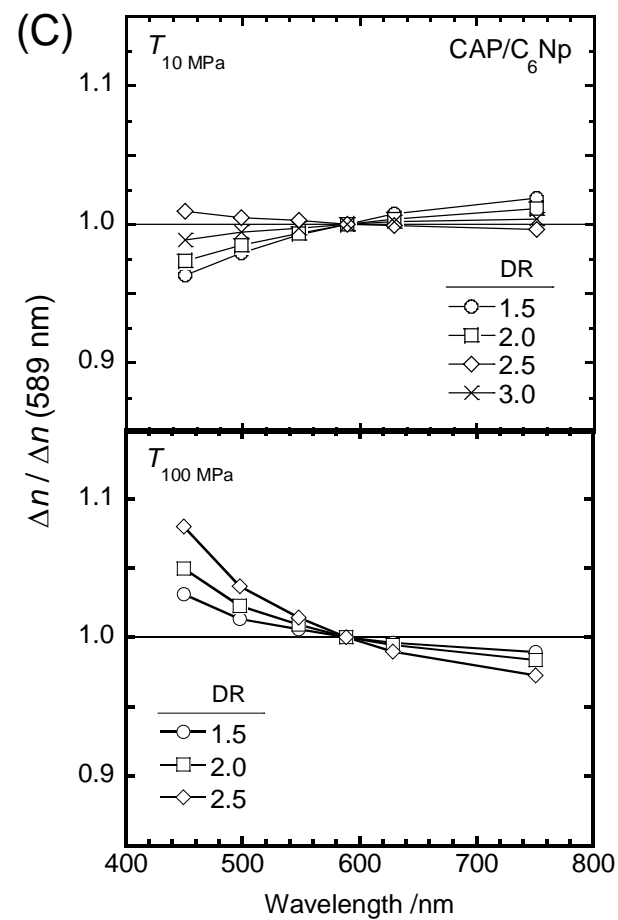
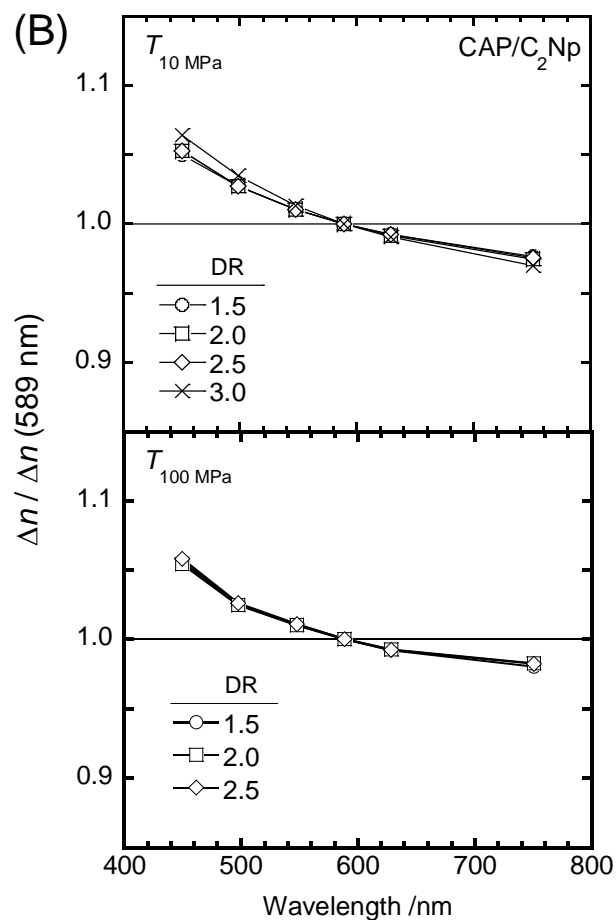
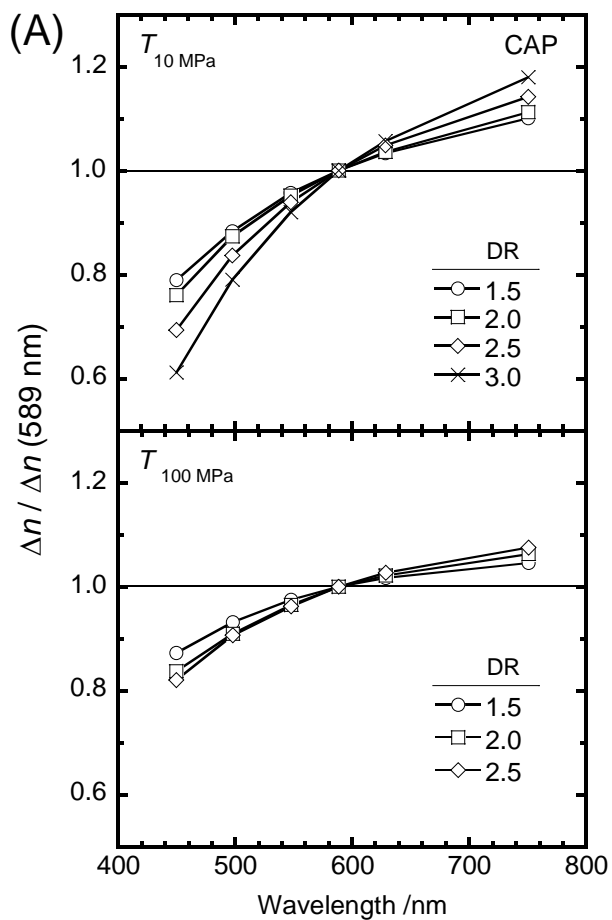


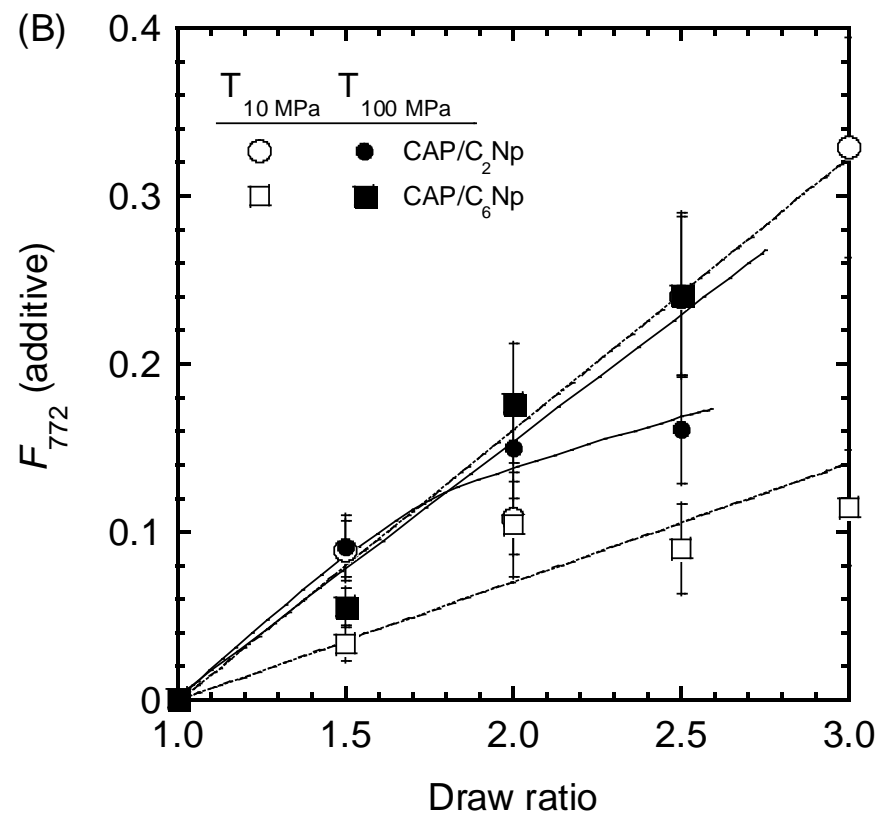
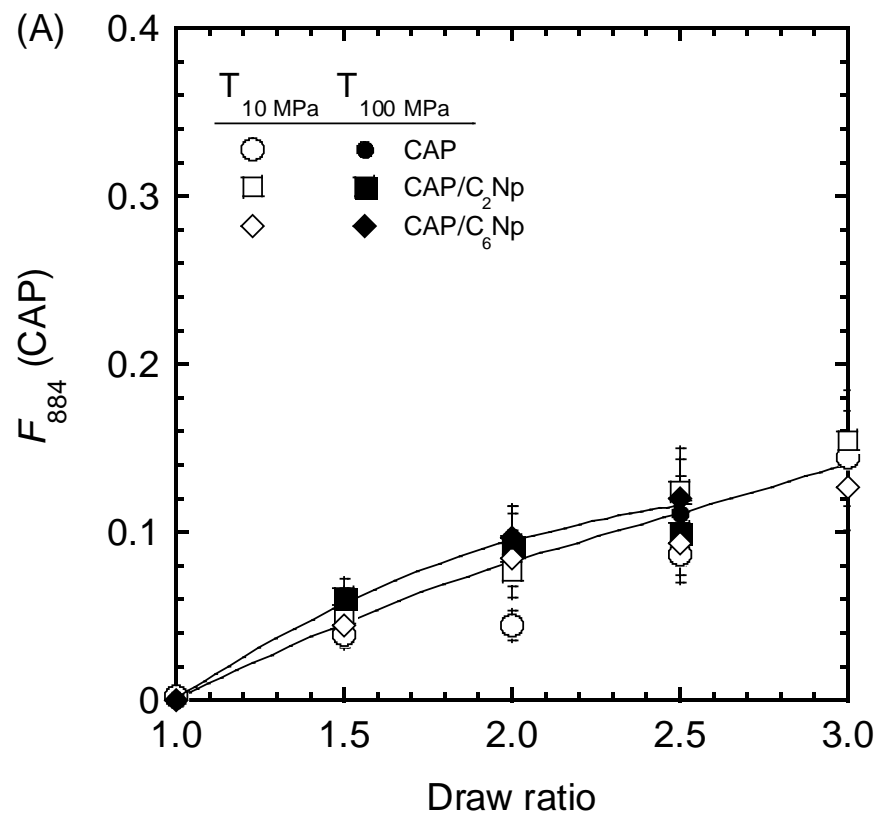


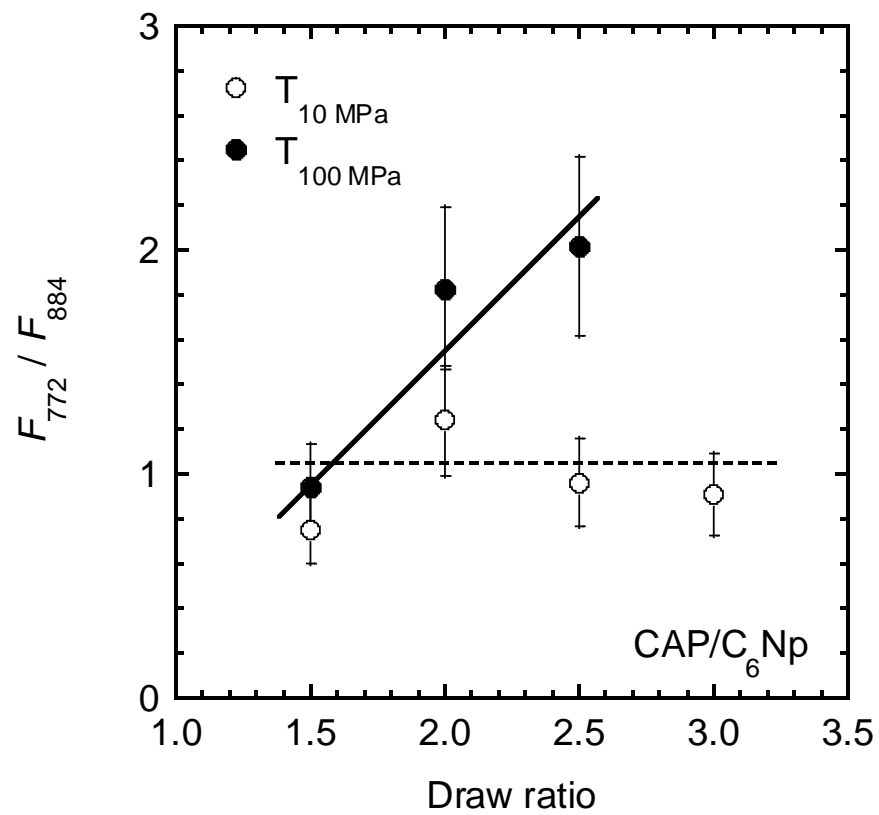
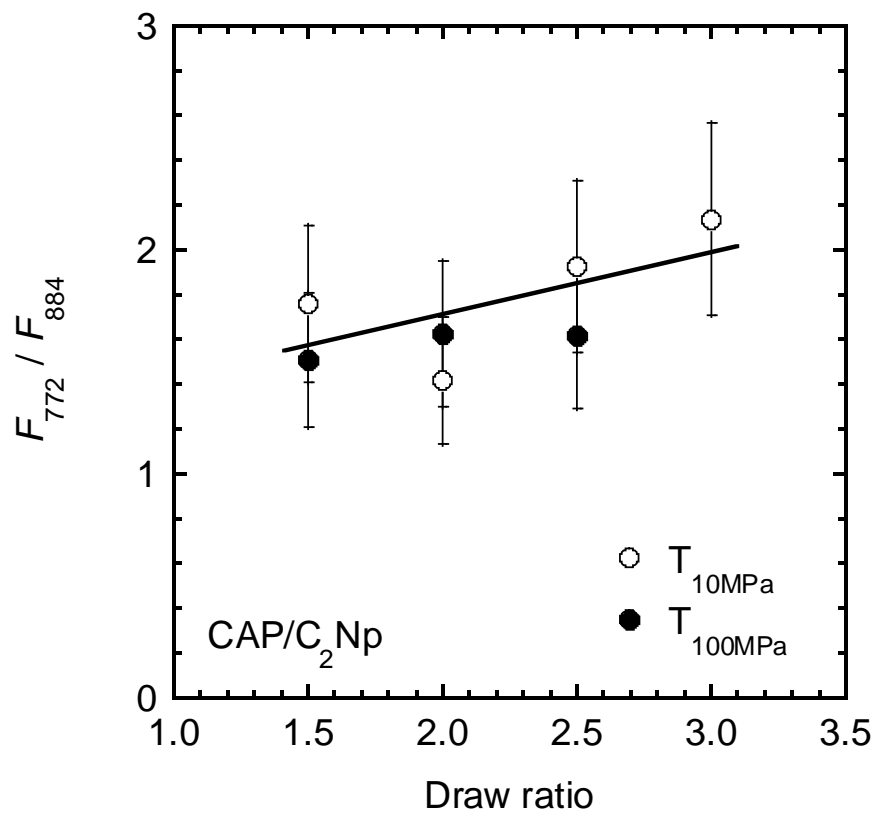




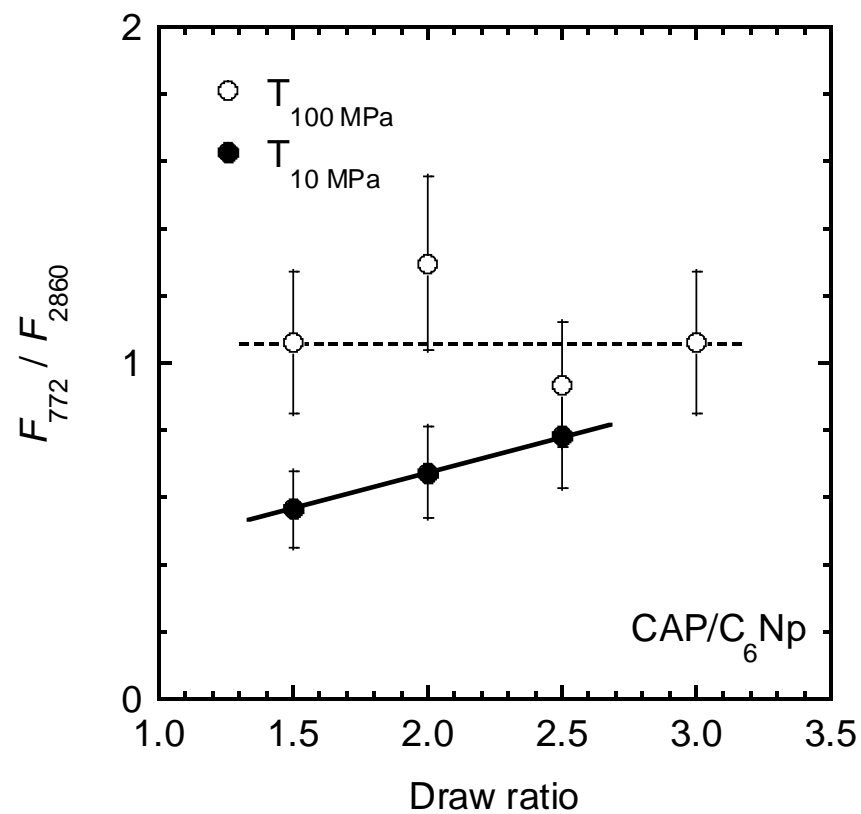












## Supplementary information

The effect of flexible chains on the orientation dynamics of small molecules dispersed in polymer films during stretching

*Shogo Nobukawa\*, Yoshihiko Aoki, Yoshiharu Fukui, Ayumi Kiyama, Hiroshi Yoshimura, Yutaka Tachikawa, and Masayuki Yamaguchi*

\*Corresponding author

Affiliation: *Japan Advanced Institute of Science and Technology, 1-1 Asahidai, Nomi, Ishikawa 923-1292, Japan,*

E-mail: nobukawa@jaist.ac.jp

**Orientation function determined by polarized FT-IR spectroscopy**

In order to evaluate the degree of orientation for CAP, C<sub>2</sub>Np and C<sub>6</sub>Np in the stretched films, polarized FT-IR spectra were measured. Intensities of absorption peaks for CAP, C<sub>2</sub>Np and C<sub>6</sub>Np were evaluated. The assignments of the peaks were summarized in Table S1.

The peak at 772 cm<sup>-1</sup> is assigned to the out-of-plane bending of the aromatic ring C-H groups for C<sub>2</sub>Np and C<sub>6</sub>Np<sup>1</sup>, while the peak at 884 cm<sup>-1</sup> are assigned to asymmetric stretching mode of a pyranose ring or wagging mode of ring C-H bonds.<sup>2,3</sup> The peak at 806 cm<sup>-1</sup> is regarded as the parallel vibration mode to the chain axis from the FT-IR data although the assignment has not been reported. Asymmetric (asym.) and symmetric (sym.) stretching vibrations for C-H in methylene group<sup>4</sup> are observed at 2800-3000 cm<sup>-1</sup> for CAP, C<sub>2</sub>Np and C<sub>6</sub>Np. The sym. stretching peak of C-H bond for C<sub>6</sub>Np at 2860 cm<sup>-1</sup> can be decomposed from that for matrix CAP at 2884 cm<sup>-1</sup>, although the asym. peaks for both components cannot be separated due to the overlapping.

The polarized FT-IR spectroscopy gives the information of molecular orientation in stretched polymer films.<sup>5</sup> Two spectra parallel and perpendicular to the stretching direction are obtained from the FT-IR measurement. Since the intensity of absorption peak is

dependent on the orientation direction of each transition moment, the dichroic ratio,  $R = A_{//} / A_{\perp}$ , is related to the orientation function,  $F$ , as follows,

$$F = \frac{R_0 + 1}{R_0 - 2} \frac{R - 1}{R + 2} \quad (\text{S1})$$

Here,  $A_{//}$  and  $A_{\perp}$  are peak intensities of polarized spectra parallel and perpendicular to the stretching direction, respectively.  $R_0 = 2\cot^2\beta$ , where  $\beta$  is the angle between the transition moment corresponding to the absorption band and the chain axis. The angle  $\beta$  for each band can be determined from the FT-IR spectra simulated along parallel and perpendicular directions to the chain axis by using density functional theory (DFT/B3LYP) with 6-31+G(d,p) basis set. As the result, the angles  $\beta$  for CAP were estimated to be 68.6 and 0° at 884 and 806 cm<sup>-1</sup>, respectively. On the other hand,  $\beta$  for C<sub>2</sub>Np and C<sub>6</sub>Np was determined to be 90° at 772 cm<sup>-1</sup>. The angle  $\beta$  for the asymmetric C-H stretching vibration is also 90° at 2840 cm<sup>-1</sup> only for C<sub>6</sub>Np.

### Analysis of the absorbance for each peak

Figures S1 and S2 show polarized FT-IR spectra for CAP and CAP/additive films as examples. As seen in Figure S1, the absorbance,  $A$ , for C-H bending vibrations of CAP, C<sub>2</sub>Np and C<sub>6</sub>Np is determined by drawing baseline. In contrast,  $A$  for C-H stretching mode of C<sub>6</sub>Np is estimated as the peak area by deconvolution of the spectrum with the sum of five Lorentz type functions represented by,

$$ABS(\nu) = \sum_i^5 \frac{A_i}{\pi} \frac{B_i}{(\nu - \nu_i)^2 + B_i^2} \quad (\text{S2})$$

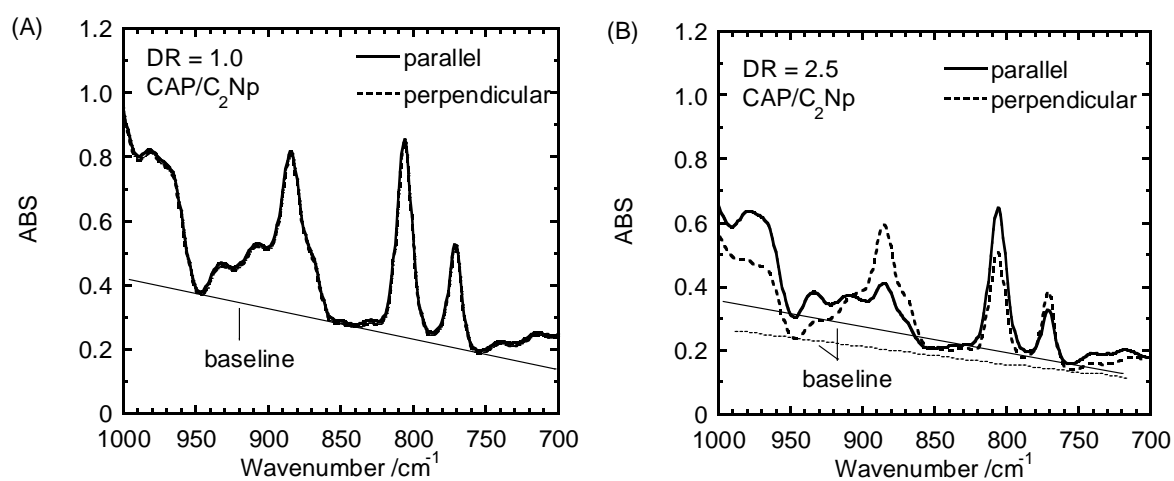
Here,  $A_i$ ,  $B_i$ , and  $\nu_i$  are surface area, half width, and absorption wavenumber for  $i$ th peak. Examples are shown in Figure S2. For the deconvolution of the spectra,  $A_i$  was a variable while  $B_i$ , and  $\nu_i$  were used as constant values. As seen in the figure, the fifth peak at 2860 cm<sup>-1</sup> is observed only in CAP/C<sub>6</sub>Np film. By applying the obtained absorbance  $A$  for each peak to equation S1, the orientation function for CAP, C<sub>2</sub>Np and C<sub>6</sub>Np can be estimated.

Table S1. Peak assignments in FT-IR spectra for CAP, C<sub>2</sub>Np and C<sub>6</sub>Np.

	out-of-plane bending	stretching or wag.	C-H stretching frequency <sup>4</sup> , $\nu / \text{cm}^{-1}$	
	aromatic C-H	of C-H (pyranose)	-CH <sub>3</sub> , asym.	-CH <sub>2</sub> -, asym. / sym.
CAP <sup>*</sup>	-	884, 806 <sup>2,3</sup>	2981	2943 / 2884
C <sub>2</sub> Np <sup>**</sup>	772 <sup>1</sup>	-	-	2956 / 2884
C <sub>6</sub> Np <sup>**</sup>	772 <sup>1</sup>	-	-	2940 / 2860

\* in bulk

\*\* in chloroform solution

Figure S1. Polarized FT-IR spectra of CAP/C<sub>2</sub>Np film (A) unstretched and (B) stretched with a draw ratio of 2.5. Baselines for evaluation of orientation functions are drawn in the figures.

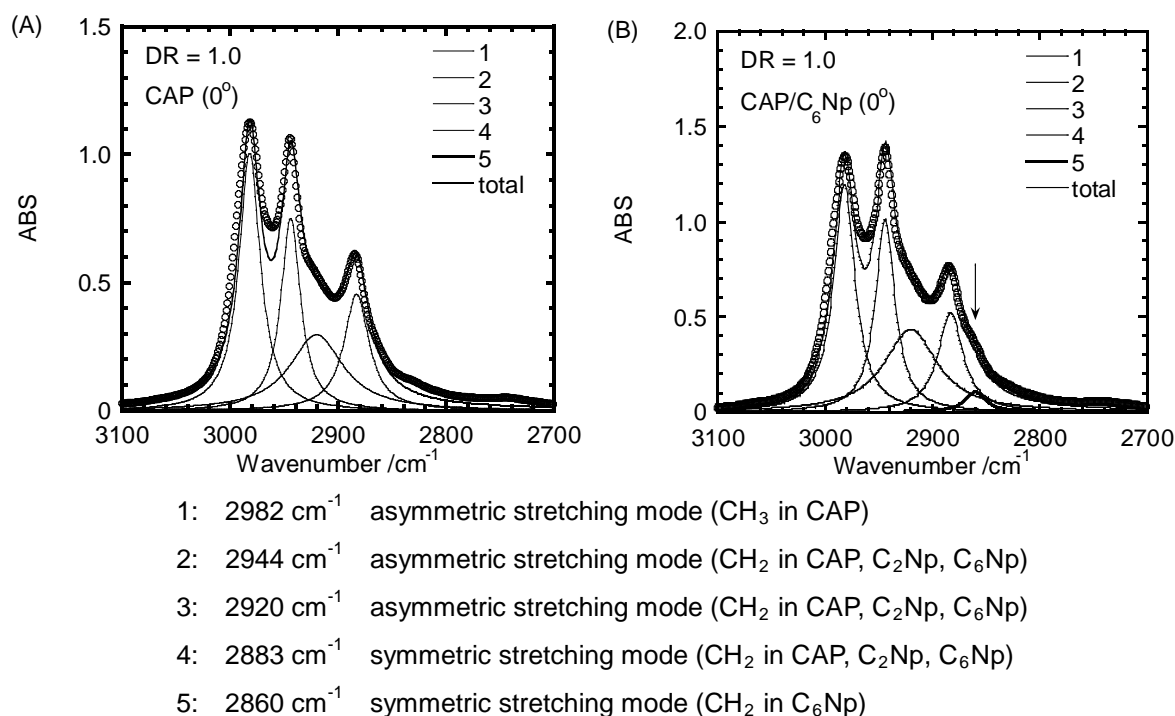


Figure S2. Deconvolution of polarized FT-IR spectra of (A) CAP and (B) CAP/C<sub>6</sub>Np films with a polarized angle = 0°. The order of peak number is from high to low wavenumber.

## References

1. Scott, A., Hakme, C., Stevenson, I. & Voice, A., Structural information on the transition moments in poly(ethylene-2,6-naphthalene) by polarization FT-IR spectroscopy. *Macromol. Symp.* **230**, 78-86 (2005).
2. Kondo, T. & Sawatari, C., A Fourier transform infra-red spectroscopic analysis of the character of hydrogen bonds in amorphous cellulose. *Polymer* **37**, 393-399 (1996).
3. Ilharco, L. M., Garcia, A. R., daSilva, J. L. & Ferreira, L. F. V., Infrared approach to the study of adsorption on cellulose: Influence of cellulose crystallinity on the adsorption of benzophenone. *Langmuir* **13**, 4126-4132 (1997).
4. Silverstein, R. M., Webster, F. X. & Kiemle, D. J., *Spectrometric Identification of Organic Compounds*. 7th ed. (ed. Silverstein, R. M., Webster, F. X. & Kiemle, D. J.) (John Wiley & Sons, Inc., New York, 2005).
5. Zhao, Y., Jasse, B. & Monnerie, L., Fourier-transform infra-red and birefringence studies of orientation in uniaxially stretched poly(methyl methacrylate)-poly(trifluoroethylene) blends. *Polymer* **32**, 209-214 (1991).